applied sciences

MDPI

Article

# Properties of Aged GFRP Reinforcement Grids Related to Fatigue Life and Alkaline Environment

**Francesco Micelli [1], Marco Corradi [2,*], Maria Antonietta Aiello [1,*] and Antonio Borri [2]**

[1] Department of Innovation Engineering, University of Salento, Via per Monteroni, 73100 Lecce, Italy; francesco.micelli@unisalento.it

[2] Department of Engineering, Perugia University, Via Duranti, 92, 06125 Perugia, Italy; antonio.borri@unipg.it

* Correspondence: marco.corradi@unipg.it (M.C.); antonietta.aiello@unisalento.it (M.A.A.); Tel.: +39-75-585-2908 (M.C.)

Received: 31 July 2017; Accepted: 30 August 2017; Published: 1 September 2017

**Abstract:** In recent years, even if Fiber Reinforced Polymer (FRP) composites have been widely used for strengthening of civil buildings, a new generation of materials has been studied and proposed for historical masonry construction. These buildings, mainly made of stone work, are common in many areas of Europe and Asia and recent earthquakes has been the cause of many catastrophic failures. The brittleness of unreinforced historic masonry can be considerably reduced using new retrofitting lighter-weight materials such FRP, even if limitations were evidenced due to material and mechanical compatibility with poor substrates. Thus, fibrous reinforcements were used as long fibres incorporated into a cement or lime matrix, which better match with the properties of ancient masonry. The use of low strength fibers such as glass and basalt, respect to carbon, in presence of an alkaline matrix brought out durability issues, due to the chemical vulnerability of common glass and basalt fibres. The objective of this research is to explore the effects of selected aqueous environments and fatigue loading on the mechanical and physical properties of composite grids, made of E-CR (Electrical/Chemical Resistance) glass fibers and epoxy-vinylester resin, used as tensile reinforcement in new composite reinforced mortar systems. Glass-fiber-reinforced polymer (GFRP) coupons were subjected to tensile testing and a severe protocol of durability tests, including alkaline environment and fatigue tensile loads. Accelerated ageing tests were used to simulate long-term degradation in terms of chemical attack and consequent reduction of tensile strength. The ageing protocol consisted of immersion at 40 °C in alkaline bath made by deionized water and $Ca(OH)_2$, 0.16% in weight, solution for 30 days. GFRP specimens aged and unaged were also tested under tensile fatigue cycles up to 1,000,000 cycles and a nominal frequency of 7.5 Hz. After this severe conditioning the tests indicate a good tensile strength retention of the GFRP in absence of fatigue loads, while a significant loss in fatigue life was experienced when both alkaline exposure and fatigue loads were applied.

**Keywords:** historic masonry; ageing; fatigue; composite materials; testing

## 1. Introduction and Research Significance

Masonry buildings are characteristic of the architectural heritage throughout most of Europe, North Africa and Asia. However, masonry constructions are notoriously vulnerable to earthquakes due to the almost total lack of tensile strength of the masonry material. Traditional methods for retrofitting and restoration of masonry constructions have sometimes demonstrated to be inappropriate: Reinforced Concrete (RC) roofs and floors, concrete jacketing of wall panels can highly enhance the structural behavior of masonry buildings, but they also produce an increment in dead loads, increase the structural stiffness reducing ductility, present problems of oxidation of steel reinforcement.

From the 1990s, there has been some movement away from traditional construction materials for retrofitting applications, toward lighter-weight solutions. The use of FRP (Fiber Reinforced Polymers)

materials are particularly suited to strengthening pre-existing masonry constructions and can be used to extend the fatigue life or provide an increase in strength of a structure [1–4].

However, there is limited guidance available on the use of FRPs in strengthening of masonry structures. The long term behavior of FRPs materials used in masonry strengthening needs to be investigated, especially when composite materials are in the form of thin sheets or grids. FRPs are usually bonded to the external surface of an existing masonry structure: bonding is often achieved using epoxy adhesives; recently, however, FRP materials has been employed also in combination with inorganic matrix such as lime mortars and cement, to fulfill new needs in retrofit of historical constructions [5–11].

In such situation, the analysis of the vulnerability of FRPs to environmental damage is critical and should be proved. The life cycle of FRPs must be competitive with traditional materials, because of the limited available resources to maintain and protect architectural heritage structures.

There are many areas where knowledge of the behavior of FRPs for masonry applications is currently lacking. Perhaps one of the more important areas is the performance of these materials under combined effects of fatigue and ageing. In this paper, a durability study has been conducted in order to investigate the residual mechanical propertied of GFRP grids subjected to exposure in alkaline bath and fatigue cycles.

The effects of fatigue have been extensively studied for many composite products [12], mainly in areas outside of civil engineering structures (automotive and aerospace engineering). However there is little information about the products used in retrofitting of masonry structures. Notoriously, fatigue failure occurs due to the application of fluctuating stresses that are lower than the stress needed to produce failure during a monotonous loading application. The study reported in [13] considered the fatigue effects in bonded regions of FRP plates used for small bridge applications, but only few information are found in terms of residual strength of the fibers [14–16] and FRP-reinforced elements [17,18]. In these studies the fatigue effects caused a reduction of the static strength as expected. An aggressive chemical environment such as high alkaline pore solution is another threat for the glass fibers, when Alkali Resistant (AR) solutions are not used. A significant degradation in modulus and strength can be produced by the chemical sensitivity of E-glass (alumino-borosilicate glass), ordinary basalt fibers and their organic matrices. According to the authors of [19,20] this can be addressed to three different mechanisms. They include the effect of free hydroxyl $OH^-$ ions and water molecules which cause corrosion of the fibers; a second effect due to the precipitation of hydration products, which may reduce the flexibility of the fibers and change the behavior at the interface with the inorganic matrix; the presence of chemical products which cause a densification of the matrix at the interface level which may produce a bending effect in the fibers.

Several studies demonstrated the vulnerability of glass fibers (mainly E-glass) by showing a reduced tensile strength after ageing [21–25]. In these studies, it has been noted that the diffusion of the $OH^-$ ions out of the glass structures (leaching) is the most common dissolution reaction of the glass material. Few studies have investigated the combination of alkaline attack with fatigue cycles [26–29]. According to the state of the art in the field, a need to expand the knowledge in the field of the long-term behavior of composite reinforcement used in civil engineering, is diffusely felt. The use of fibers which may meet harsh environment and potentially detrimental chemical agents should be investigated. The possible combination of mechanical and chemical agents meets a strong interest in the research community for the provision of design guidelines. According to this needs and aiming to expand the frontiers of the knowledge in the field, this study presents durability evaluations to provide new information in the field. The results of an experimental program are presented and discussed, showing the residual tensile properties of GFRP materials subjected to alkaline exposure and fatigue loading.

## 2. GFRP Specimens and Ageing Protocol

The GFRP reinforcement that was investigated in this experimental research is industrially produced in forms of 0°/90° grids, starting from glass fibers yarns that are impregnated at a temperature of 120 °C. The spacing of the grids in both direction is 66 mm (see Figure 1). Each strand of fibers used as raw material is made by four filaments having a TEX of 2400 each. From a chemical point of view the fibers used are E-CR-glass (Electrical/Chemical Resistance) which are basically E-glass fibers modified by the presence of alumino-lime silicate which reduce the chemical vulnerability in alkaline environment.

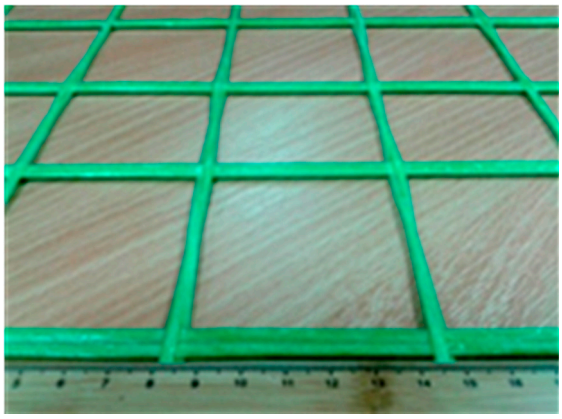

**Figure 1.** Glass-fiber-reinforced polymer (GFRP) grid with a 66 × 66 mm mesh size.

The matrix used for the impregnation was an epoxy-vinylester resin. Due to the used technology, the fibers amount is not the same in the two directions. The GFRP net presents a different geometry in the two directions, since the fibers are cured in forms of a flat plate in 0° direction and in forms of a twisted cord in 90° direction (see Figure 2). The effective amount of fibrous reinforcement in the cross section was quantified by applying two different methods: (1) the technique recommended by the technical guidelines CNR-DT 203 [30], ACI 440.3R [31], ISO 10406-1 [32], which consists of a measurement by using a graduated cylinder; (2) an hydrostatic weighting by measuring the volume of the specimens, which is an alternative method that have higher accuracy. This because the use of the first technique may be affected by an uncertainty that undergoes from 20 to 40%. It is expressed as percentage of the average value of the measuring sample. The use of the second technique may reduce the uncertainty which is in the range of 1–2%. By using the first method the equivalent cross section was respectively 8.9 (flat) and 6.6 $mm^2$ (twisted); by using the second method the equivalent cross section was respectively 9.2 $mm^2$ (flat) and 6.7 $mm^2$ (twisted).

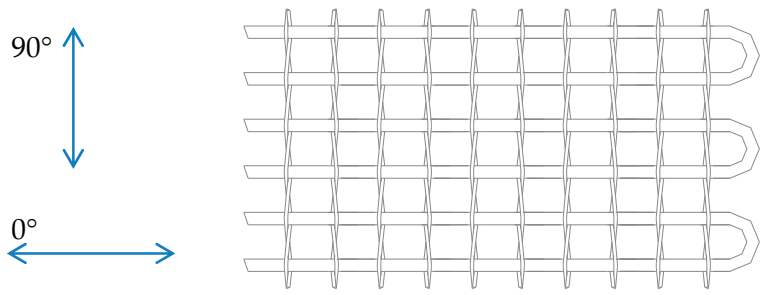


(**a**)

**Figure 2.** *Cont.*

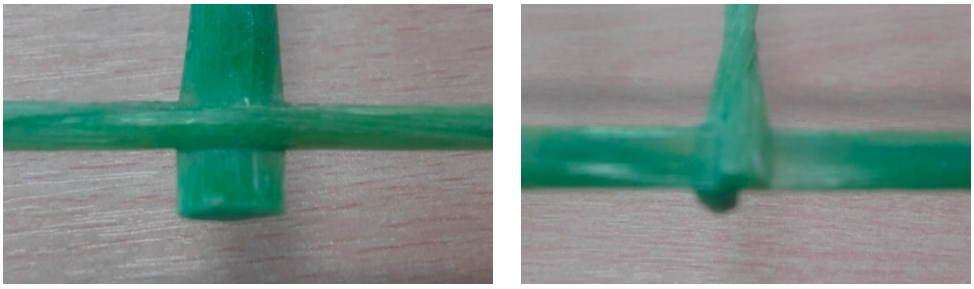

(**b**) (**c**)

**Figure 2.** Different reinforcement bars: (**a**) schematic layout; (**b**) flat bar (0°); (**c**) twisted bar (90°).

In order to detect the effects of alkaline pore solutions, which may arise within lime mortars in presence of high humidity, an aggressive aqueous solution was prepared as ageing bath. The specimens were immersed for 718 h in an alkaline aqueous solution made by a 0.16% (weight) of $Ca(OH)_2$, simulating a lime-based environment. The target pH of the solution was 12.6, which was monitored during the exposure period as shown in Figure 3. A controlled temperature of 40 ± 2 °C was maintained in the thermostatic bath during the exposure period in order to accelerate the diffusion effects of the aggressive solution inside the GFRP.

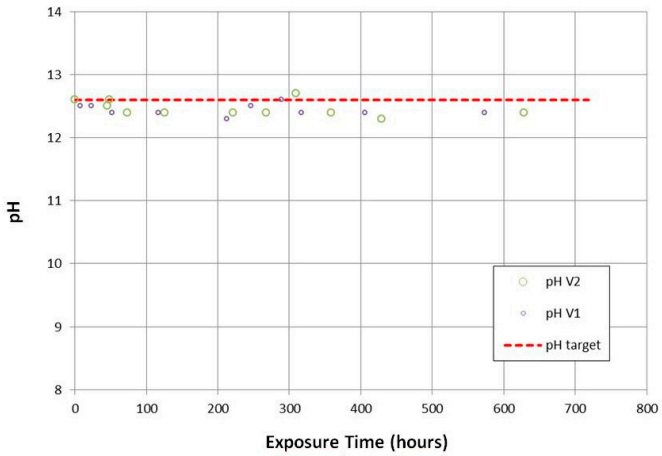


**Figure 3.** Experimental pH level during exposure.

The constant temperature of the solution was produced and ensured by using two containers (identified as "tank 1" and "tank 2", with a capacity of 120 L and 100 L respectively) which were placed inside a close box in which the heated bottom acted as heating unit. The uniformity of the temperature in the cabinet was optimized using a ventilation system (internal recirculation), also below the bottom of containers. After an initial period of 300 h (during which the temperatures were always within the expected rank of 40 ± 2 °C), a constant temperature has been assured by implementing a solution recirculation between the two containers, with a flow of 0.5% /min (recirculation of 0.5% of the total solution volume in 1 min).

The temperature was monitored using a thermometer at different locations and depths in the two containers and recording the maximum and minimum values detected. Additionally, the monitoring was also made in correspondence of the surface by using another thermometer.

A correlation between the real service life and the period of accelerated ageing in laboratory (days) was provided for a cementitious environments in [33], as a first hypothesis this correlation may be considered also valid for the presented case:

$$\frac{N}{C} = 0.098 \times e^{0.0558 \times T} \quad (1)$$

where:

$N$ = age in natural days
$T$ = conditioning temperature expressed in °F
$C$ = number of days of accelerated exposure at temperature T

The typical aspect the GFRP specimens after alkaline exposure is illustrated in Figure 4. After the artificial exposure in alkaline environment, corresponding to 2.66 years in real conditions according to Equation (1), the aged specimens were washed with water and dried at room temperature (21 °C). The drying was performed under a forced air oven without increasing the temperature in order to avoid post-cure effects which may modify the real results. A white coating is visible on the surface of the GFRP grids after exposure, which is due to the precipitated products produced by the presence of the alkaline ions.

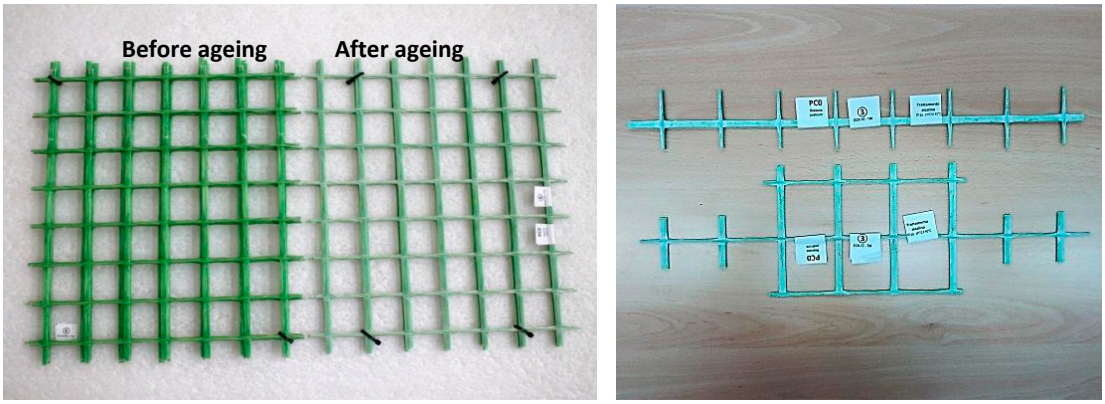


(**a**) (**b**)

**Figure 4.** GFRP grids after exposure in alkaline bath. (**a**) Comparison between aged and unaged grid; (**b**) Aged specimens.

## 3. Testing Program

The lack of a validated and comprehensive data base for the durability of GFRP grids as related to reinforcement applications for masonry structures has been recognized as a critical barrier to the use of these composite materials. In this study environments of interest are alkalinity and fatigue effects. For many masonry structures subject to cyclic loading (for example bridge structures, smokestacks and slender towers), ageing and fatigue are an important limit state that must be considered in the design process. When embedded into a lime- or cement-based mortar, GFRP grids come in contact with alkaline media. To study the potential effects (hydrolysis, pitting, hydroxylation, etc.) of degradation due to mortar pore water solution, GFRP specimens were first aged in alkaline solution and subsequently subjected to tension-tension axial fatigue tests. In this research the fatigue protocol resulted much more severe than those situations detected in real service conditions, but this allowed to better highlight the sensitivity respect to this type of ageing.

In this study the specimens that were investigated respect to long-term properties were cut from the GFRP grids along the 0° direction, meaning that the tensile properties were measured for the flat GFRP bars (see Figure 2a). In the following all the descriptions and results are related to the flat bars.

Firstly mechanical tests were performed to measure the tensile properties of the GFRP specimens, such as tensile strength, elastic modulus and ultimate strain. Tensile tests were also performed after the ageing/fatigue protocols. Tensile tests were run firstly on twenty unconditioned specimens, which provided the characterization of the GFRP materials, without any mechanical and chemical ageing.

The preliminary tensile tests were run by using a Zwick Roell universal testing machine, having a capacity of 100 kN. Tensile tests were run under displacement control with a controlled rate equal to 0.2 mm/min, at a room temperature of 23 °C and relative humidity of 50%. An electric extensometer was used to measure the strain. ASTM D3039 [34] standard was used as reference for static tests. Furthermore ten specimens were cut from the same grid, subjected only to the alkaline ageing protocol, and tested under an uniaxial monotonic tensile force as same as done for reference specimens, without any fatigue treatment. This was done in order to detect the chemical sensitivity in presence of alkaline ions, and in absence of any other agent or harsh environment.

Then a set of sixteen specimens was cut from the same GFRP grid of the unconditioned specimens, to be subjected to fatigue loads with and without previous alkaline exposure. Totally eight specimens were subjected to alkaline exposure before the fatigue cycles, while the other eight were fatigued without any chemical ageing.

Fatigue tests were performed on a servo-hydraulic E3000 Instron machine (Instron, Norwood, MA, USA) with a 3 kN capacity load cell. Surface temperature was monitored using a voltmeter with a sensibility of 0.15 °C. The load amplitude and test frequency of the fatigue treatment were constant (1.0 kN and 7.5 Hz, respectively). Tests were conducted at a room temperature of 21 °C in stress control using a normalized maximum tensile stress ($\sigma_{max}/\sigma_{ult}$) of approx. 0.25, 0.35, 0.45 and 0.55 (corresponding to maximum tensile loads of 1, 1.5, 2, and 2.5 kN). Table 1 summarizes the experimental program of tensile static tests, while in Table 2 the fatigue test protocol is illustrated, including the number of specimens tested, the maximum fatigue load and number of scheduled cycles. In Figures 5 and 6 the fatigue machine and the loading histories used in this study are illustrated.

**Table 1.** Monotonic tensile tests matrix. NT for unconditioned and AG for aged specimens.

| Number of Specimens | Labels | Treatment | Grid Directions |
|---|---|---|---|
| 30 | 1NT–20NT | Unconditioned | 0° - flat |
| 10 | 1AG–10AG | Alkaline bath | 0° - flat |

**Table 2.** Fatigue tests matrix. F was used for those specimens that were subjected to fatigue loads.

| Specimen | Treatment | Grid Directions | Maximum Load of Fatigue Treatment (kN) | Number of Scheduled Cycles |
|---|---|---|---|---|
| 1NT-F<br>2NT-F | Unconditioned | 0° - flat | 2.5 | 1,000,000 |
| 3AG-F<br>4AG-F | Alkaline bath | 0° - flat | 2.5 | 1,000,000 |
| 5NT-F<br>6NT-F | Unconditioned | 0° - flat | 2 | 1,000,000 |
| 7AG-F<br>8AG-F | Alkaline bath | 0° - flat | 2 | 1,000,000 |
| 9NT-F<br>10NT-F | Unconditioned | 0° - flat | 1.5 | 1,000,000 |
| 11AG-F<br>12AG-F | Alkaline bath | 0° - flat | 1.5 | 1,000,000 |
| 13NT-F<br>14NT-F | Unconditioned | 0° - flat | 1 | 1,000,000 |
| 15AG-F<br>16AG-F | Alkaline bath | 0° - flat | 1 | 1,000,000 |

For fatigue tests, GFRP specimens were dry cut from the grid with final dimensions of approx. 190 mm using a diamond saw. A clear distance between grips of approximately 90 mm was used.

The specimen shape was bar form and, within the length of the GFRP specimens, two grid joints were included as the grid spacing was 66 mm.

Strength and modulus degradation was studied by performing monotonic tensile static tests at the end of the ageing and fatigue treatments, for those specimens which did not fail before the scheduled cycles number. In total, thirty specimens were tested under uniaxial tension without fatigue loads, while totally sixteen specimens were subjected to fatigue loads; four specimens that did not fail during the fatigue tests were subjected to further tensile tests until failure.

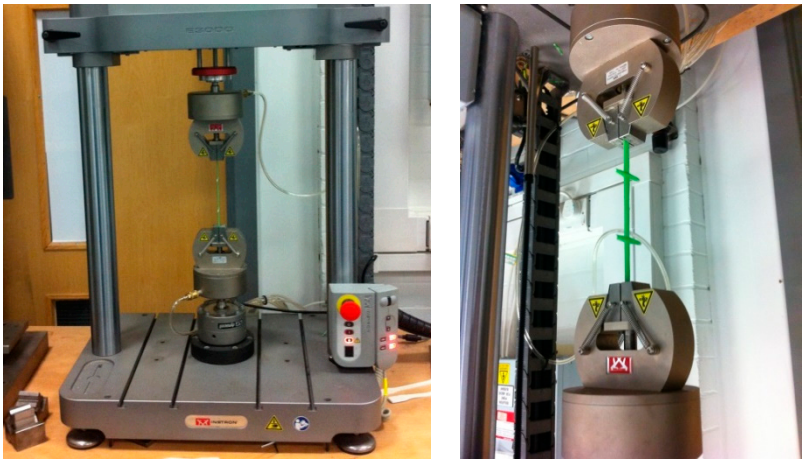

(**a**) (**b**)

**Figure 5.** Fatigue testing (**a**) Fatigue testing machine; (**b**) GFRP specimen under test.

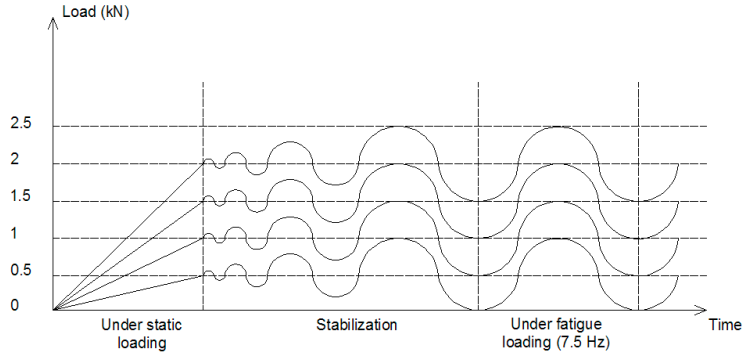


**Figure 6.** Test protocol for fatigue cycles with different amplitudes.

An alphanumeric code was used for sample identification (ID). This was made of a progressive number ranging from 1 to 16 and a two-letter designation (NT for unconditioned and AG for aged specimens). The final letter F was used for those specimens that were subjected to fatigue loads.

## 4. Experimental Results

The results presented herein will show how the tensile strength and the Young's modulus were affected by comparing results that were obtained, for specimens subjected to alkaline ageing, fatigue cycles, fatigue cycles and alkaline ageing and unconditioned ones.

### *4.1. Tensile Tests of Unconditioned and Aged Specimens*

The experimental results related to the tensile properties for a total number of 20 unconditioned reference specimens are shown in Table 3. As it can been observed the standard deviation and

coefficient of variation are within a range of about 10% for the elastic modulus and about 20% for the tensile strength. This can be considered compatible with the experimental error. The typical failure modes and details of fiber breakage are reported in Figure 7.

**Table 3.** Tensile tests results for unconditioned specimens.

| Specimen | Young's Modulus E (GPa) | Ultimate Load $P_{ult}$ (kN) | Tensile Strength $\sigma_{ult}$ (MPa) | Elongation at Failure (%) | Cross Section ($mm^2$) |
|---|---|---|---|---|---|
| 1NT | 21.47 | 5.05 | 546.75 | 2.4 | 9.2 |
| 2NT | 28.77 | 4.78 | 517.21 | 1.8 | 9.2 |
| 3NT | 29.11 | 4.58 | 495.45 | 1.7 | 9.2 |
| 4NT | 31.78 | 3.79 | 410.06 | 1.3 | 9.2 |
| 5NT | 30.76 | 5.64 | 610.28 | 2.0 | 9.2 |
| 6NT | 23.85 | 5.08 | 549.57 | 2.3 | 9.2 |
| 7NT | 29.80 | 4.09 | 443.07 | 1.5 | 9.2 |
| 8NT | 32.13 | 4.95 | 535.28 | 1.7 | 9.2 |
| 9NT | 31.34 | 4.66 | 504.76 | 1.6 | 9.2 |
| 10NT | 31.76 | 3.21 | 347.08 | 1.5 | 9.2 |
| 11NT | 30.31 | 6.36 | 688.64 | 2.3 | 9.2 |
| 12NT | 26.44 | 5.17 | 559.85 | 2.0 | 9.2 |
| 13NT | 26.64 | 4.88 | 527.71 | 1.9 | 9.2 |
| 14NT | 28.86 | 4.89 | 529.33 | 1.8 | 9.2 |
| 15NT | 33.05 | 3.46 | 374.78 | 1.2 | 9.2 |
| 16NT | 32.30 | 6.28 | 679.87 | 2.2 | 9.2 |
| 17NT | 31.56 | 3.70 | 400.87 | 1.3 | 9.2 |
| 18NT | 27.78 | 3.62 | 391.77 | 1.4 | 9.2 |
| 19NT | 29.94 | 3.66 | 396.21 | 1.3 | 9.2 |
| 20NT | 31.90 | 5.49 | 594.26 | 1.9 | 9.2 |
| Average Value | 29.48 | 4.67 | 505.14 | 1.76 | 9.2 |
| Standard Deviation | 3.00 | 0.91 | 98.03 | 0.37 | - |
| COV (%) | 10.19 | 19.41 | 19.41 | 21.04 | - |

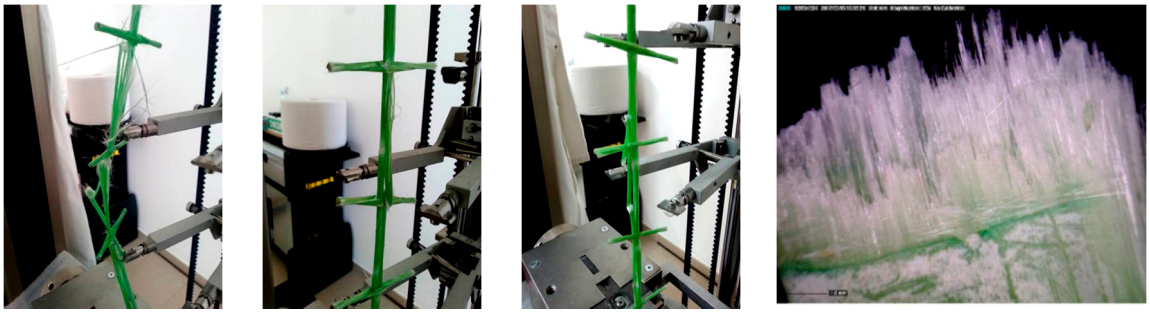

(**a**) (**b**) (**c**) (**d**)

**Figure 7.** Typical tensile failures of GFRP specimens. (**a**) and (**b**) near the joint; (**c**) tensile failure; (**d**) detail of the specimen's section after tensile failure.

In all cases the tensile failure of the fibers was accompanied by an intra-laminar cracking occurred in the polymeric matrix that developed along the direction of the applied load. The breakage of the glass fibers occurred in different positions, even if the complete failure was mainly located in those regions nearby the nodal junctions. The stress-elongation behavior is linear or pseudo-linear up to failure, as shown in Figure 8.

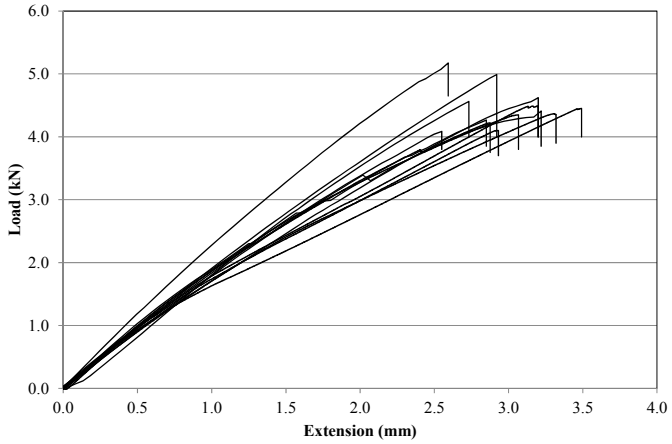


**Figure 8.** Typical stress-elongation curves for GFRP tested specimens.

Aged specimens subjected to alkaline environment exhibited the same failure modes and the same linear behavior in terms of stress–strain curves. The elastic modulus and ultimate tensile properties are shown in Table 4.

**Table 4.** Tensile tests results for aged specimens in alkaline bath.

| Specimen | Young's Modulus E (GPa) | Ultimate Load $P_{ult}$ (kN) | Tensile Strength $\sigma_{ult}$ (MPa) | Elongation at Failure (%) | Cross Section ($mm^2$) |
|---|---|---|---|---|---|
| 1AG | 30.39 | 4.20 | 454.33 | 1.5 | 9.2 |
| 2AG | 30.62 | 4.81 | 521.00 | 1.8 | 9.2 |
| 3AG | 29.54 | 3.37 | 364.61 | 1.2 | 9.2 |
| 4AG | 27.63 | 2.79 | 302.38 | 1.2 | 9.2 |
| 5AG | 30.77 | 3.44 | 372.51 | 2.2 | 9.2 |
| 6AG | 30.16 | 4.17 | 450.97 | 1.5 | 9.2 |
| 7AG | 29.59 | 4.57 | 494.81 | 1.7 | 9.2 |
| 8AG | 31.11 | 4.12 | 445.67 | 1.5 | 9.2 |
| 9AG | 30.39 | 3.37 | 364.29 | 1.2 | 9.2 |
| 10AG | 30.62 | 3.48 | 376.84 | 1.6 | 9.2 |
| Average Value | 30.08 | 3.83 | 414.74 | 1.54 | 9.2 |
| Standard Deviation | 0.99 | 0.63 | 68.67 | 0.31 | - |
| COV (%) | 3.30 | 16.56 | 16.56 | 20.35 | - |

Also in this case the standard deviation and coefficient of variation values were maintained within the range of the experimental error. From a comparison between aged and reference specimens no reduction was found in terms of elastic modulus, while a slight reduction of 18% was found in terms of tensile strength. This can be attributed to the weakening of the fibers that were put in contact with the alkaline ions, and at the same time to the damage of the matrix that was not totally impermeable to the diffusion of the harsh aqueous solution.

The diffusion of alkaline ions and the breaking of the Si-O-Si bond, which is the main structure of the glass fiber, causes the damage of the fibers. The degradation mechanisms affecting glass fibers are different and combined. A filament corrosion due to $OH^-$ ions may occur, moreover a sort of static fatigue can cause the breaking due to the growth of existing surface defects, related to the $OH^-$ ions attack, furthermore a growth of densification products due to the precipitation of crystals in the interstices between the filaments of the fiber may cause a localized damage. Static fatigue failure is the most common mode. In general, fiberglass damage is closely related to the chemical composition of the alkaline solution to which it is subject. As for the matrix, it is important that it does not undergo degradation in such a way as to protect and transmit the loads to the fibers. However, the matrix, if subjected to alkaline solution, may undergo plasticization and/or swelling due to its diffusion inside, resulting in a reduction in the matrix's ability to perform its role. After the performance of this testing

program, even if a reduction of mechanical properties was expected, it is felt that the tested specimens have shown a high retention of the mechanical properties, which are strongly related to the design values that should be assumed in the long-term.

### 4.2. Specimens Subjected to Tension–Tension Fatigue

The results of the fatigue tests are presented in this section in terms of number of cycles to failure and residual life of GFRP. In Table 5 the fatigue test results are illustrated, in addition to the tensile strength that was measured under monotonic load for those specimens that did not fail after the final loading history ($10^6$ cycles). From Table 5 it can be noted that only for a small quantity of GFRP specimens the number of scheduled loading cycles was completed. The most part of specimens, both aged or unconditioned, failed in tension during the fatigue cycles. However, some interesting observations can be raised.

**Table 5.** Fatigue tests results of reference and aged GFRP.

| ID | Treatment in Alkaline Bath | Maximum Fatigue Load (kN) | Number of Cycles at Failure | Ultimate Load (kN) | Residual Tensile Strength (MPa) |
|---|---|---|---|---|---|
| 1NT-F | Unconditioned | 2.5 | 50,553 | - | - |
| 2NT-F | | 2.5 | 38,546 | - | - |
| 3AG-F | Alkaline bath | 2.5 | 26,942 | - | - |
| 4AG-F | | 2.5 | 23,539 | - | - |
| 5NT-F | Unconditioned | 2 | no rupture | 1.17 | 127.17 |
| 6NT-F | | 2 | 163,088 | - | - |
| 7AG-F | Alkaline bath | 2 | 28,045 | - | - |
| 8AG-F | | 2 | 232,661 | - | - |
| 9NT-F | Unconditioned | 1.5 | 638,157 | - | - |
| 10NT-F | | 1.5 | 111,779 | - | - |
| 11AG-F | Alkaline bath | 1.5 | 98,026 | - | - |
| 12AG-F | | 1.5 | 62,466 | - | - |
| 13NT-F | Unconditioned | 1 | no rupture | 3.12 | 339.13 |
| 14NT-F | | 1 | no rupture | 3.86 | 416.56 |
| 15AG-F | Alkaline bath | 1 | 410,988 | - | - |
| 16AG-F | | 1 | no rupture | 5.54 | 602.17 |

The failure modes in the broken cross sections were similar to the failure modes of the static experiments carried out on unconditioned specimens: all failures occurred in the area around the joint, demonstrating the small deviations of glass fibers from the direction of the tensile load may represent a critical defect. Glass fibers in both grid directions 0°/90° have to deviate in the joint area and this may produce significant reductions in tensile strength. Furthermore, the tensile failures were brittle without announcement by large deformations or visible cracks on the specimen surfaces. In Table 6 representative failed specimens and failure details are illustrated for GFRP specimens failed under the application of the fatigue cycles.

Of particular interest was the number of loading cycles sustained before failure. In fact, the number of loading cycles before failure has been used to indicate the mechanical degradation. Results were obtained for a range of loading cycles between 23,539 and 638,157. It is evident that the GFRP specimens are sensitive to the tension-tension fatigue treatment. The most part of aged specimens sustained a lower number of loading cycles before tensile failure, compared to unconditioned specimens, indicating a degradation effect. The stress–strain response was almost linear-elastic in the load range used for fatigue testing.

Furthermore, when tension-tension fatigue tests had a lower maximum load, GFRP specimens could sustain a larger number of loading cycles, indicating the significant effects of the fatigue test. In detail, only unconditioned specimens with a maximum fatigue load of 1 kN (corresponding to a

normalized maximum tensile stress ($\sigma_{max}/\sigma_{ult}$ of approximate 0.25) completed the scheduled number of cycles.

Because GFRP specimens were made of a organic polymeric matrix with elastic glass fibers, the typical degradation, commonly designated as plasticity for metals, cannot occur. However other irreversible mechanisms may be activated during a fatigue test, such as matrix cracking and fiber/matrix debonding. From the experimental data it was seen that fatigue load up to 1.0 kN did not produce important degradation. After fatigue test the static tensile test for specimens 13NT-F and 14NT-F monotonic tests showed an ultimate tensile load that was comparable with that of unconditioned specimens. For the unique specimen that was fatigued up to 2.0 kN, remaining unbroken, the residual tensile strength strongly decreased up to about the 25% of the reference GFRP specimen. The specimen 16AG-F can be considered as a singularity result since the residual strength is located in the maximum quartile of the strength values of the reference GFRP specimens. In all cases it is strongly felt that the peak load in the fatigue history plays a decisive role in determining the residual life of the tested GFRP reinforcement.

**Table 6.** Failure modes of unaged and aged GFRP under fatigue loads.

| Specimen | Failure Mode | Damage Details | Specimen | Failure Mode | Damage Details |
|---|---|---|---|---|---|
| | **Unconditioned** | | | **Alkaline Aged** | |
| 1NT-F | 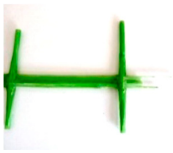 | 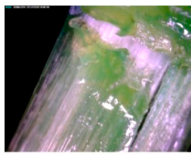 | 3AG-F | 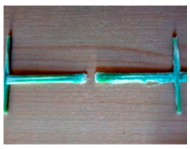 | 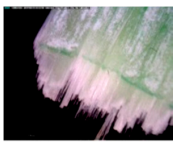 |
| 2NT-F | 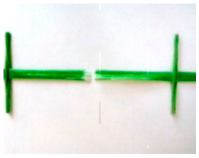 | 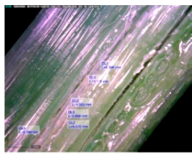 | 4 AG-F | 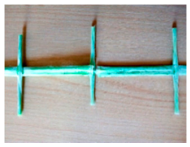 | 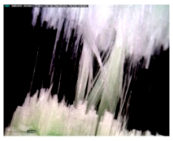 |
| 6NT-F |  | 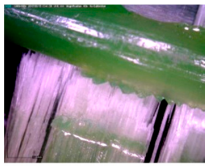 | 7AG-F |  |  |
| 9NT-F | 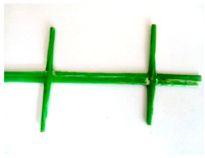 | 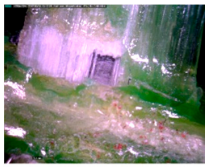 | 11AG-F | 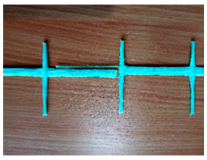 | 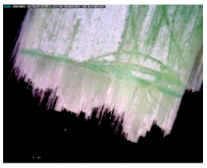 |
| 10NT-F |  | 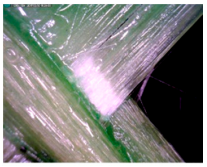 | 12AG-F | 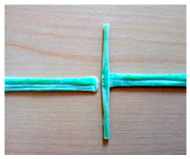 | 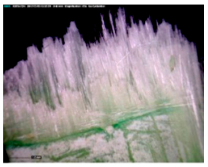 |

## 5. Conclusions

The results of an experimental program that studied the durability of GFRP reinforcement respect to alkaline environment and fatigue loads were presented and discussed in the paper. Coupons cut from GFRP pre-cured grids made by ECR glass fibers and epoxy-vinylester matrix were tested as reference and aged coupons. Alkaline ageing and fatigue loads were studied alone and in combination to each other. Severe protocols were applied to emphasize the sensitivity of the tested materials to the studied chemical and mechanical agents.

After conditioning in alkaline bath with pH 12.6 for 718 h at 40 °C it was found that the loss in terms of elastic modulus was negligible, while the maximum reduction in terms of residual strength was 18%. In this perspective the tested GFRP have exhibited a high chemical strength.

When fatigue loads were applied it was seen that the maximum load level applied during the fatigue tension-tension cycles played a significant role. The number of cycles up to failure significantly decreased when the maximum loads up to 2.5 kN were applied. For peak loads of 1.0 kN it was seen that unaged specimens were able to show a residual life, and a slight reduction of about 25% was found in terms of tensile strength respect to the reference GFRP specimens. The combination of fatigue and alkaline ageing was found to be very detrimental, since the fatigue life, in general, decreased after alkaline exposure. This because the micromechanical damage due to the chemical attack is strongly enhanced by the presence of cyclic loads.

Future research is needed in the field, even if it is felt that important information are provided to researchers and practitioners through the results presented herein.

**Acknowledgments:** The authors thank L. Calabrese, M. Dundas and L. Amess for assistance which made this work possible. Northumbria University partially provided the funding which made this research possible through the internal support funds. Furthermore the support of FibreNet in developing the presented research is strongly appreciated by the authors.

**Author Contributions:** Marco Corradi, Francesco Micelli, Antonio Borri and Maria Antonietta Aiello conceived and designed the experiments; Marco Corradi and Francesco Micelli performed the experiments and analyzed the data; Marco Corradi and Francesco Micelli wrote the paper under the supervision of Antonio Borri and Maria Antonietta Aiello.

**Conflicts of Interest:** The authors declare no conflict of interest.

## References

1. Babaeidarabad, S.; De Caso, F.; Nanni, A. URM walls strengthened with fabric-reinforced cementitious matrix composite subjected to diagonal compression. *J. Compos. Constr.* **2013**, *18*, 68–70. [CrossRef]
2. Gattesco, N.; Amadio, C.; Bedon, C. Experimental and numerical study on the shear behavior of stone masonry walls strengthened with GFRP reinforced mortar coating and steel-cord reinforced repointing. *Eng. Struct.* **2015**, *90*, 143–157. [CrossRef]
3. Corradi, M.; Borri, A.; Castori, G.; Sisti, R. Shear strengthening of wall panels through jacketing with cement mortar reinforced by GFRP grids. *Compos. Part B Eng.* **2014**, *64*, 33–42. [CrossRef]
4. Castori, G.; Borri, A.; Corradi, M. Behavior of thin masonry arches repaired using composite materials. *Compos. Part B Eng.* **2015**, *87*, 311–321. [CrossRef]
5. Valluzzi, M.R.; Oliveira, D.V.; Caratelli, A.; Castori, G.; Corradi, M.; de Felice, G.; Garbin, G.; Garcia, D.; Garmendia, L.; Grande, E.; et al. Round robin test for composite-to-brick shear bond characterization. *Mater. Struct.* **2012**, *45*, 1761–1791. [CrossRef]
6. Maljaee, H.; Ghiassi, B.; Lourenço, P.B.; Oliveira, D.V. FRP—Brick masonry bond degradation under hygrothermal conditions. *Compos. Struct.* **2016**, *147*, 143–154. [CrossRef]
7. Maljaee, H.; Ghiassi, B.; Lourenço, P.B.; Oliveira, D.V. Moisture-induced degradation of interfacial bond in FRP-strengthened masonry. *Compos. Part B Eng.* **2016**, *87*, 47–58. [CrossRef]
8. Raoof, S.M.; Bournas, D.A. Bond between TRM versus FRP composites and concrete at high temperatures. *Compos. Part B Eng.* **2017**, *127*, 150–165. [CrossRef]
9. Sciolti, M.S.; Aiello, M.A.; Frigione, M. Effect of thermo-hygrometric exposure on FRP, natural stone and their adhesive interface. *Compos. Part B Eng.* **2015**, *80*, 162–176. [CrossRef]
10. Ghiassi, B.; Xavier, J.; Oliveira, D.V.; Lourenço, P.B. Application of digital image correlation in investigating the bond between FRP and masonry. *Compos. Struct.* **2013**, *106*, 340–349. [CrossRef]
11. Garzón-Roca, J.; Sena-Cruz, J.M.; Fernandes, P.; Xavier, J. Effect of wet-dry cycles on the bond behaviour of concrete elements strengthened with NSM CFRP laminate strips. *Compos. Struct.* **2015**, *132*, 331–340. [CrossRef]
12. Tong, J. Characteristics of fatigue crack growth in GFRP laminates. *Int. J. Fatigue* **2002**, *24*, 291–297. [CrossRef]
13. Keller, T.; Tirelli, T. Fatigue behavior of adhesively connected pultruded GFRP profiles. *Compos. Struct.* **2003**, *65*, 55–64. [CrossRef]

14. El-Assal, A.M.; Khashaba, U.A. Fatigue analysis of unidirectional GFRP composites under combined bending and torsional loads. *Compos. Struct.* **2007**, *7*, 599–605. [CrossRef]
15. Andersons, J.; Korsgaard, J. Residual strength of GFRP at high-cycle fatigue. *Mech. Compos. Mater.* **1999**, *35*, 395–402. [CrossRef]
16. Demers, C.E. Tension—Tension axial fatigue of E-glass fibre reinforced polymeric composites: Fatigue life diagram. *Constr. Build. Mater.* **1998**, *12*, 303–310. [CrossRef]
17. Borri, A.; Castori, G.; Corradi, M.; Sisti, R. Masonry wall panels with GFRP and steel-cord strengthening subjected to cyclic shear: An experimental study. *Constr. Build. Mater.* **2014**, *56*, 66–73. [CrossRef]
18. Brena, S.F.; Benouaich, M.A.; Kreger, M.E.; Wood, S.L. Fatigue tests of reinforced concrete beams strengthened using carbon fiber-reinforced polymer composites. *ACI Struct. J.* **2005**, *102*, 305–313.
19. Bentur, A.; Mindess, S. *Fibre Reinforced Cementitious Composites*, 2nd ed.; CRC Press: Boca Raton, FL, USA, 2006.
20. Majumdar, A.J.; Laws, V. *Glass Fibre Reinforced Cement*; BSP Professional Books: Oxford, UK, 1991.
21. Chu, W.; Wu, L.; Karbhari, V.M. Durability evaluation of moderate temperature cured E-glass/vinylester systems. *Compos. Struct.* **2004**, *66*, 367–376. [CrossRef]
22. Micelli, F.; Nanni, A. Durability of FRP rods for concrete structures. *Constr. Build. Mater.* **2004**, *18*, 491–503. [CrossRef]
23. Chen, Y.; Davalos, J.F.; Ray, I.; Kim, H.Y. Accelerated aging tests for evaluations of durability performance of FRP reinforcing bars for concrete structures. *Compos. Struct.* **2007**, *78*, 101–111. [CrossRef]
24. Karbhari, V.M.; Chin, J.W.; Hunston, D.; Benmokrane, B.; Juska, T.; Morgan, R.; Lesko, J.J.; Sorathia, U.; Reynaud, D. Durability gap analysis for Fiber-Reinforced Polymer composites in civil infrastructure. *J. Compos. Constr. ASCE* **2003**, *7*, 238–247. [CrossRef]
25. Chen, Y.; Davalos, J.F.; Ray, I. Durability prediction for GFRP reinforcing bars using short-term data of accelerated aging tests. *J. Compos. Constr. ASCE* **2006**, *10*, 279–286. [CrossRef]
26. Earl, J.S.; Shenoi, R.A. Hygrothermal ageing effects on FRP laminate and structural foam materials. *Compos. Part A* **2004**, *35*, 1237–1247. [CrossRef]
27. Corradi, M.; Righetti, L.; Osofero, A.I.; Borri, A.; Castori, G.; Sisti, R. Accelerated aging and fatigue effects on GFRP grids. In Proceedings of the sixth Congress on Collapses, Structural Reliability and Strengthening (IF CRASC 2015), Rome, Italy, 14–16 May 2015; pp. 455–466.
28. Micelli, F.; Aiello, M.A. Residual tensile strength of dry and impregnated reinforcement fibres after exposure to alkaline environments. *Compos. Part B Eng.* **2017**, in press. [CrossRef]
29. Calabrese, L.; Micelli, F.; Corradi, M.; Aiello, M.A.; Borri, A. Ageing and fatigue combined effects on GFRP grids. *Key Eng. Mater.* **2017**, *747*, 525–532. [CrossRef]
30. CNR-DT 203/2006. *CNR-DT 203/2006 Guide for the Design and Construction of Concrete Structures Reinforced with Fiber-Reinforced Polymer Bars*; ROME—CNR: Rome, Italy, 2007.
31. ACI 440.3R/2004. *Guide Test Methods for Fiber-Reinforced Polymers (FRPs) for Reinforcing or Strengthening Concrete Structures*; American Concrete Institute: Farmington Hills, MI, USA, 2004.
32. ISO 10406-1/2008. *Fibre-Reinforced Polymer (FRP) Reinforcement of Concrete—Test Methods*; ISO: Geneva, Switzerland, 2008.
33. Litherland, K.L.; Oakley, D.R.; Proctor, B.A. The use of accelerated aging procedures to predict the long term strength of GRF composites. *Cement Concr. Res.* **1981**, *11*, 455–466. [CrossRef]
34. ASTM D3039/2014. *Standard Test Method for Tensile Properties of Polymer Matrix Composite Materials*; ASTM: West Conshohocken, PA, USA, 2014.